

Weak antilocalization in two-dimensional systems with large Rashba splitting

L. E. Golub,¹ I. V. Gornyi,^{1,2} and V. Yu. Kachorovskii¹

¹*Ioffe Institute, St. Petersburg 194021, Russia*

²*Institut für Nanotechnologie, Karlsruhe Institute of Technology, 76021 Karlsruhe, Germany*

We develop the theory of weak localization for two-dimensional electrons with a large, linear-in-momentum Rashba or Dresselhaus spin-orbit splitting. Assuming a short-range disorder potential, we derive analytical expressions for the quantum conductivity correction in both diffusive and ballistic regimes. For zero magnetic field, we identify a ballistic contribution to the quantum correction which is not sensitive to the details of scattering and dephasing, and depends only on the spectrum properties. Further, we calculate the magnetoconductivity in the whole range of classically weak magnetic fields and find that it is negative for an arbitrary relation between the Fermi energy and the spin-orbit splitting. We show that the magnetoconductivity changes with the Fermi energy when the Fermi level is above the “Dirac point” and saturates when the Fermi level goes below this point.

PACS numbers: 73.20.Fz, 73.61.Ey

I. INTRODUCTION

Weak localization is a coherent phenomenon in the low-temperature transport in disordered systems. Transport in random media is realized by various trajectories, including a special class of trajectories with closed loops. The underlying physics of the weak localization is the coherent enhancement of the backscattering amplitude which results from the constructive interference of the waves propagating along such loops in the opposite directions (clockwise and counterclockwise). Since interference increases the backscattering amplitude, quantum conductivity correction is negative and is proportional to the ratio of the de Broglie wavelength to the mean free path [1]. Remarkably, this correction diverges logarithmically at low temperatures in the two-dimensional (2D) case. Such a divergency is a precursor of the strong localization and reflects universal symmetry properties of the system.

Dephasing processes suppress interference and, consequently, strongly affect the conductivity correction. Specifically, the typical size of interfering paths is limited by the time of electron dephasing, τ_ϕ . At low temperatures, the dephasing rate is dominated by inelastic electron-electron collisions. The phase space for such collisions decreases with lowering temperature. Therefore, one can probe dephasing processes by measuring the temperature dependence of conductivity in the weak-localization regime [2]. Another possibility to affect the interference-induced quantum correction to the conductivity is application of magnetic field. The Aharonov-Bohm effect introduces a phase difference for the waves traveling along the closed loop in the opposite directions. This phase difference equals to a double magnetic flux passing through the loop. The anomalous magnetoconductivity allows one to extract the dephasing time even more accurately than the temperature measurements since the low-field magnetoconductivity is not masked by other effects [1, 3].

Since weak localization is caused by the interference

of paths related to each other by time inversion, it is extremely sensitive to spin properties of interfering particles. In systems with spin-orbit coupling, an additional spin-dependent phase is acquired by electrons passing the loops clock- and anti-clockwise. As a result, the interference depends on the electron spin states before and after passing the loop. At strong spin-orbit coupling, the interference is not constructive but destructive, resulting in a positive correction to the conductivity. This interference effect is called weak antilocalization. Magnetic field suppresses this correction making the conductivity smaller than in zero field, i.e. the magnetoconductivity is negative [1].

Theory of weak localization developed in 1980’s for diffusive systems allowed one to explain a number of experimental data in various metallic and semiconductor structures [2]. Spin-orbit interaction has been treated as spin relaxation which adds an additional channel for dephasing of the triplet contributions to the quantum corrections [1]. However, this approach is insufficient for 2D semiconductor heterostructures where the spin-orbit interaction results in a splitting of energy spectrum linear in the electron momentum. The relevant theory of weak localization has been developed in the middle of 1990’s [4]. It describes very well experimental data [5, 6].

The increasing quality of heterostructures with high electron mobility resulted in observation of anomalous magnetoconductivity in the field range where the magnetic length l_B is comparable to or even smaller than the mean free path l . This regime of weak localization can not be treated within the model of a diffusive electron motion along large scattering paths. By contrast, the interference is realized in a so-called ballistic regime at small paths with a few scatterers [7–9]. The anomalous magnetoconductivity in this regime has been calculated in Refs. [7, 9] which allowed one to fit the experimental data [10]. The same problem in high-mobility heterostructures with spin-orbit splitting has been solved in Refs. [11, 12] which allowed describing the weak-antilocalization data in various high-mobility

heterostructures [12, 13].

The spin-orbit splitting in the theory [12] was assumed to be comparable to or even larger than the momentum scattering rate \hbar/τ , see Fig. 1. The spin dynamics can be well described by electron spin rotations in the effective momentum-dependent magnetic field [14, 15]. However, when the spin-orbit splitting becomes of the order of the Fermi energy, effects of spin-orbit interaction on the electron orbital motion can not be neglected in the calculation of the conductivity correction. Recently, 2D systems have become available where such a ultra-strong splitting can be realized. Examples are electrons near the surface of polar semiconductors and at LAO/STO interfaces, or holes in HgTe-based quantum well structures with a large spin-orbit splitting [16–18]. In this regime, the spin energy branches are well separated (see Fig. 1, right panel), which results in strongly coupled dynamics of electron spin and orbital degrees of freedom. The classical conductivity then shows substantial deviations from the usual Drude transport law [19]. Weak localization for well-separated spin branches has been considered in Ref. [20, 21] in the diffusive regime and in zero magnetic field only. Recently, weak localization in spin-orbit metals based on the HgTe quantum wells has been examined in the model of double-degenerate branches of the massive Dirac fermions [22–26].

In the present work, we develop a theory of weak localization for the systems with an arbitrary large splitting of spin branches. We study the quantum interference in the presence of short-range disorder potential which provides effective inter-branch scattering. We consider contributions to the anomalous magnetoconductivity from an arbitrary number of scatterers and derive expressions valid in both diffusion and ballistic regimes of weak localization.

The paper is organized as follows. In Section II we formulate the model. In Section III we present the derivation of the interference-induced conductivity correction. In Section IV, the results for the magnetoconductivity and the zero-field correction are presented and discussed. Section V summarizes our conclusions.

II. MODEL

The Hamiltonian of 2D electrons has the form

$$H = \frac{\hbar^2 k^2}{2m} + \alpha(\boldsymbol{\sigma} \times \mathbf{k})_z, \quad (1)$$

where \mathbf{k} is a two-dimensional momentum, z is a normal to the structure, m is the effective mass, $\boldsymbol{\sigma}$ is a vector of Pauli matrices, and α is the Rashba constant. The isotropic energy spectrum consists of two branches enumerated by the index $s = \pm$:

$$E_s(k) = \frac{\hbar^2 k^2}{2m} + s\alpha k \quad (2)$$

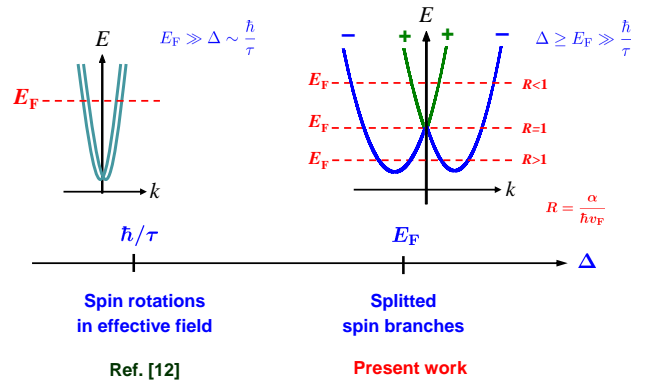


FIG. 1. Regimes of spin dynamics at various strength of the Rashba splitting.

with the splitting $\Delta = 2\alpha k$, Fig. 1. It is worth noting that the same spectrum describes electrons with a \mathbf{k} -linear isotropic 2D Dresselhaus spin-orbit interaction [15, 27] with the substitution of α by the 2D Dresselhaus constant. The eigenfunctions in the two branches are spinors $\Psi_{s,\mathbf{k}} = (1, -ise^{i\varphi_{\mathbf{k}}})/\sqrt{2}$ with $\varphi_{\mathbf{k}}$ being the polar angle of \mathbf{k} .

The spectrum (2) is approximately linear in the vicinity of $k = 0$, where the \pm bands touch each other (see Fig. 1, right panel). In what follows, we will term this special point the “Dirac point”. We will first consider the situation when the Fermi energy is located above the Dirac point. In this case, the eigenstates at the Fermi level belong to two different branches.

Disorder leads to the following types of scattering processes: intra-branch ($++$ and $--$) and inter-branch ($+-$ and $-+$). In this paper we consider short-range disorder, so that the scattering matrix element between the states s, \mathbf{k} and s', \mathbf{k}' is given by

$$V_{s's} = V_0 \Psi_{s',\mathbf{k}'}^\dagger \Psi_{s\mathbf{k}} = V_0(1 + ss'e^{-i\theta})/2, \quad (3)$$

where a constant V_0 is the strength of the short-range scattering potential, and $\theta = \varphi_{\mathbf{k}'} - \varphi_{\mathbf{k}}$ is the scattering angle. Importantly, the short-range potential provides effective inter-branch scattering for an arbitrary spin-orbit splitting. The total (quantum) scattering rate is the same in both branches:

$$\frac{1}{\tau} = \frac{2\pi}{\hbar} \langle |V_{++}|^2 g_+ + |V_{+-}|^2 g_- \rangle_\theta = \frac{m}{\hbar^3} V_0^2. \quad (4)$$

Here the angular brackets denote averaging over θ , and the densities of states at the Fermi energy in the branches are given by

$$g_\pm = \frac{m}{2\pi\hbar^2} (1 \mp R). \quad (5)$$

The parameter R is introduced according to

$$R = \frac{\alpha}{mv_F}, \quad (6)$$

where v_F is the Fermi velocity equal in both branches.

In contrast to the quantum scattering rates, the transport rates in the branches are different. In order to calculate the transport times, we solve a system of equations for the velocity vertexes in the subbands, v_s^x :

$$v_s^x(\varphi) = v_F \cos \varphi + \sum_{s'=\pm} (1-s'R) \left\langle \frac{1+ss'\cos\theta}{2} v_{s'}^x(\varphi') \right\rangle_{\varphi'}. \quad (7)$$

The solution is given by $v_s^x(\varphi) = v_F \cos \varphi \tau_{\text{tr}}^s/\tau$, where

$$\frac{\tau_{\text{tr}}^\pm}{\tau} = 1 \mp R. \quad (8)$$

The scattering rates for Fermi energy located below the Dirac point ($R > 1$) are discussed in Sec. III B.

III. CONDUCTIVITY CALCULATION

We investigate two cases when the Fermi level is above and below the Dirac point, Fig. 1. We start with the first case, corresponding to $R < 1$.

A. Fermi level above the Dirac point

The retarded (R) and advanced (A) Green functions in the subband s are given by

$$G_s^{R,A}(\mathbf{r}, \mathbf{r}') = G_0^{R,A}(\mathbf{r}, \mathbf{r}'; k_F^s) \frac{1}{2} \begin{pmatrix} 1 & \pm i s e^{-i\phi} \\ \mp i s e^{i\phi} & 1 \end{pmatrix}. \quad (9)$$

Here $G_0^{R,A}(\mathbf{r}, \mathbf{r}'; k_F)$ is the standard Green function in a simple band with the Fermi wavevector k_F , k_F^s are the wavevectors at the Fermi level in two subbands, and ϕ is the polar angle of the vector $\mathbf{R} = \mathbf{r} - \mathbf{r}'$.

The weak-localization correction to the conductivity is expressed via the Cooperon. In the basis of states with spin projections on the z axis, $\alpha, \beta, \gamma, \delta = \uparrow, \downarrow$, the Cooperon satisfies the following equation:

$$\mathcal{C}_{\gamma\delta}^{\alpha\beta}(\mathbf{r}_1, \mathbf{r}_2) = [P^2(\mathbf{r}_1, \mathbf{r}_2)]_{\gamma\delta}^{\alpha\beta} + \int d\mathbf{r} P_{\gamma\nu}^{\alpha\mu}(\mathbf{r}_1, \mathbf{r}) \mathcal{C}_{\nu\delta}^{\mu\beta}(\mathbf{r}, \mathbf{r}_2), \quad (10)$$

where $P_{\gamma\nu}^{\alpha\mu}(\mathbf{r}_1, \mathbf{r}) = V_0^2 G_{\alpha\mu}^R(\mathbf{r}_1, \mathbf{r}) G_{\gamma\nu}^A(\mathbf{r}_1, \mathbf{r})$.

Under the condition $|k_F^+ - k_F^-| v_F \tau \gg 1$, which we assume from now on, the product $G_s^R(\mathbf{r}_1, \mathbf{r}) G_{s'}^A(\mathbf{r}_1, \mathbf{r})$ oscillates rapidly on the scale of the mean-free path if $s \neq s'$. Therefore P has only two terms in the sum with $s = s'$:

$$P_{\gamma\nu}^{\alpha\mu}(\mathbf{r}_1, \mathbf{r}) = V_0^2 \sum_{s=\pm} (G_s^R)_{\alpha\mu} (G_s^A)_{\gamma\nu}. \quad (11)$$

Summation over s yields the 16 components of the matrix P . Passing to the basis of states with a fixed total angular momentum and its projection to the z axis, i.e. to the basis $\uparrow\uparrow, (\uparrow\downarrow + \downarrow\uparrow)/\sqrt{2}, (\uparrow\downarrow - \downarrow\uparrow)/\sqrt{2}, \downarrow\downarrow$ we obtain that the triplet state with the zero momentum projection, i.e.

$(\uparrow\downarrow + \downarrow\uparrow)/\sqrt{2}$, does not contribute to weak localization. The matrix P corresponding to the three other states, $\uparrow\uparrow, (\uparrow\downarrow - \downarrow\uparrow)/\sqrt{2}, \downarrow\downarrow$, has the following form:

$$P = P_0 \begin{pmatrix} \frac{1}{2} & -i\frac{R}{\sqrt{2}}e^{-i\phi} & \frac{1}{2}e^{-2i\phi} \\ i\frac{R}{\sqrt{2}}e^{i\phi} & 1 & i\frac{R}{\sqrt{2}}e^{-i\phi} \\ \frac{1}{2}e^{2i\phi} & -i\frac{R}{\sqrt{2}}e^{-i\phi} & \frac{1}{2} \end{pmatrix}, \quad (12)$$

where

$$P_0(\mathbf{r}, \mathbf{r}') = \frac{\exp(-|\mathbf{r} - \mathbf{r}'|/\tilde{l})}{2\pi l |\mathbf{r} - \mathbf{r}'|} e^{i\Phi(\mathbf{r}, \mathbf{r}')}, \quad (13)$$

with $\Phi(\mathbf{r}, \mathbf{r}') = (y + y')(x' - x)/l_B^2$, $l_B = \sqrt{\hbar/|eB|}$, $e < 0$ is the electron charge, and $\tilde{l} = l/(1 + \tau/\tau_\phi)$. Here we used the fact that τ and $l = v_F \tau$ are the same in both branches.

The Cooperon can be found in the basis of Landau level states with charge $2e$. The corresponding infinite system of linear equations can be block-diagonalized in the basis of states with fixed $N + s_z$. Here $N = 0, 1, 2, \dots$ is the Landau level number, and $s_z = 1, -1$ is the angular momentum projection in the triplet state while $s_z = 0$ enumerates the singlet. The corresponding equation has the following form:

$$\mathcal{C}(N) = A_N^2 + A_N \mathcal{C}(N), \quad (14)$$

where

$$A_N = \begin{pmatrix} \frac{1}{2}P_{N-2} & i\frac{R}{\sqrt{2}}P_{N-2}^{(1)} & \frac{1}{2}P_{N-2}^{(2)} \\ i\frac{R}{\sqrt{2}}P_{N-2}^{(1)} & P_{N-1} & -i\frac{R}{\sqrt{2}}P_{N-1}^{(1)} \\ \frac{1}{2}P_{N-2}^{(2)} & -i\frac{R}{\sqrt{2}}P_{N-1}^{(1)} & \frac{1}{2}P_N \end{pmatrix}. \quad (15)$$

Here $P_N^{(m)}$ ($m = 1, 2$) and $P_N \equiv P_N^{(0)}$ are defined as follows:

$$P_N^{(m)} = \frac{l_B}{l} \sqrt{\frac{N!}{(N+m)!}} \times \int_0^\infty dx \exp(-xl_B/\tilde{l} - x^2/2) x^m L_N^m(x^2) \quad (16)$$

with L_N^m being the Laguerre polynomials. All values with negative indexes should be substituted by zeros.

The conductivity correction is a sum of two contributions:

$$\sigma = \sigma_{\text{bs}} + \sigma_{\text{non-bs}}.$$

The backscattering contribution to the magnetoconductivity is given by

$$\sigma_{\text{bs}} = \frac{\hbar}{4\pi} \int d\mathbf{r} \int d\mathbf{r}' \sum_{\alpha\beta} \left[\tilde{\mathcal{C}}(\mathbf{r}, \mathbf{r}') \Gamma(\mathbf{r}, \mathbf{r}') \right]_{\beta\alpha}^{\alpha\beta}, \quad (17)$$

where $\tilde{\mathcal{C}} = \mathcal{C} - P^2$ is the Cooperon calculated starting from three scattering lines. The squared electric current vertex is presented by the following operator

$$\Gamma = \sum_{s=\pm} \left(\frac{iel}{\hbar} \frac{\tau_{\text{tr}}^{(s)}}{\tau} \right)^2 G_s^R G_s^A. \quad (18)$$

Comparing with Eq. (11), we see that operator Γ has a matrix form similar to P , the only modification is caused by the squared transport time. As a result, we obtain:

$$\sigma_{\text{bs}}(B) = -\frac{e^2}{2\pi^2\hbar} (1 + 3R^2) \left(\frac{l}{l_B} \right)^2 \times \sum_{N=0}^{\infty} \text{Tr} \left[\Pi \tilde{A}_N A_N^2 (\mathcal{I} - A_N)^{-1} \right], \quad (19)$$

where \mathcal{I} is a 3×3 unit matrix,

$$\Pi = \text{diag}(1, -1, 1), \quad (20)$$

and \tilde{A}_N is obtained from the matrix A_N by the substitution

$$R \rightarrow R \frac{3 + R^2}{1 + 3R^2}. \quad (21)$$

The non-backscattering contribution reads:

$$\sigma_{\text{non-bs}} = \frac{\hbar}{\pi} \times \sum_{\alpha\beta} \int d\mathbf{r} \int d\mathbf{r}' \int d\mathbf{r}'' [K(\mathbf{r}, \mathbf{r}') \mathcal{C}(\mathbf{r}', \mathbf{r}'') K(\mathbf{r}'', \mathbf{r})]_{\beta\alpha}^{\alpha\beta}. \quad (22)$$

Here the vertex is given by

$$K(\mathbf{r}, \mathbf{r}') = \frac{iel}{\hbar} \sum_{s=\pm} \frac{\tau_{\text{tr}}^{(s)}}{\tau} V_0^2 G_s^R(\mathbf{r}, \mathbf{r}') G_s^A(\mathbf{r}, \mathbf{r}') \cos(\varphi - \varphi'), \quad (23)$$

where φ and φ' are polar angles of the vectors \mathbf{r} and \mathbf{r}' , respectively. Summation over s yields

$$K(\mathbf{r}, \mathbf{r}') = \frac{iel}{\hbar} \cos(\varphi - \varphi') (1 + R^2) P(R'), \quad (24)$$

where $P(R')$ is given by P , Eq. (12), with R replaced by

$$R' = \frac{2R}{1 + R^2}. \quad (25)$$

In the basis of Landau level states with charge $2e$ and fixed $N + s_z$, the operator $K(\mathbf{r}, \mathbf{r}')$ is written as

$$K = \frac{1}{2} K_N^T - \frac{1}{2} K_{N+1}, \quad (26)$$

where the matrix K_N is

$$K_N = \begin{pmatrix} \frac{1}{2} P_{N-2}^{(1)} & -i \frac{R'}{\sqrt{2}} P_{N-2}^{(2)} & \frac{1}{2} P_{N-2}^{(3)} \\ i \frac{R'}{\sqrt{2}} P_{N-1} & P_{N-1}^{(1)} & i \frac{R'}{\sqrt{2}} P_{N-1}^{(2)} \\ -\frac{1}{2} P_{N-1}^{(1)} & -i \frac{R'}{\sqrt{2}} P_N & \frac{1}{2} P_N^{(1)} \end{pmatrix}. \quad (27)$$

Finally, we obtain

$$\sigma_{\text{non-bs}}(B) = \frac{e^2}{4\pi^2\hbar} (1 + R^2)^2 \left(\frac{l}{l_B} \right)^2 \times \sum_{N=0}^{\infty} \text{Tr} \left[K_N \Pi K_N^T A_N (\mathcal{I} - A_N)^{-1} + K_N^T \Pi K_N A_{N+1} (\mathcal{I} - A_{N+1})^{-1} \right]. \quad (28)$$

B. Fermi level below the Dirac point

In this case, the Fermi contour also consists of two concentric circles, “1” and “2”, but they both belong to the outer spin branch $s = -$, Fig. 1. The Green functions in the branches are different due to unequal values of the Fermi wavevectors $k_F^{(1,2)}$. Therefore we have

$$P(\mathbf{r}, \mathbf{r}') = V_0^2 \sum_{i=1,2} G_i^R(\mathbf{r}, \mathbf{r}') G_i^A(\mathbf{r}, \mathbf{r}'). \quad (30)$$

The products $G_i^R G_i^A$ have the same coordinate dependence as at the Fermi level above the Dirac point; the difference is only in the density of states factors $g_i = k_F^{(i)}/(2\pi\hbar v_F)$ (the Fermi velocities in the branches are equal). As a result, $P(\mathbf{r}, \mathbf{r}')$ has the same form as in a one-subband system with $s = -$ with the density of states equal to $g_1 + g_2 = m/(\pi\hbar^2)$. The conductivity correction in such a system is the same as in the single branch $s = -$ with $R = 1$ and the transport time $\tau_{\text{tr}} = 2\tau$. Therefore, the corrections σ_{bs} and $\sigma_{\text{non-bs}}$ are given by Eqs. (19), (28) with $R = 1$.

The above consideration shows that the conductivity correction at $R > 1$ is equal to that at $R = 1$. In other words, when the Fermi level goes down through the Dirac point at $k = 0$, the correction does not change with further decreasing the Fermi energy to the bottom of the conduction band.

IV. RESULTS AND DISCUSSION

Let us now discuss the obtained expressions for the conductivity corrections. We remind the reader that Eqs. (19) and (28) have been obtained under the condition $|k_F^+ - k_F^-| v_F \tau \gg 1$. At small Rashba splitting relative to the Fermi energy, $R \rightarrow 0$, the derived conductivity corrections coincide with the result obtained in the limit of fast spin rotations $\Delta\tau/\hbar \rightarrow \infty$ in Refs. [11, 12].

At the Fermi level lying exactly in the Dirac point, $R = 1$, our results pass into the expressions obtained in Ref. [28] for topological insulators with a single Dirac cone. A single cone result for the considered two-subband system at $R = 1$ follows from the zero density of states of the subband $s = +$ (the Fermi wavevector for it is equal

to zero). In this case, the contribution to the conductivity of this subband is zero and scattering to it from the other branch is absent. Therefore the subband $s = +$ is excluded from transport while the states in the other branch ($s = -$) are described by the same spinors as in topological insulators.

At zero field, the conductivity corrections are given by

$$\sigma_{\text{bs}}(0) = -\frac{e^2}{8\pi^2\hbar}(1+3R^2) \int_0^\infty dx \text{Tr} \left[\Pi \tilde{A}_x A_x^2 (\mathcal{I} - A_x)^{-1} \right], \quad (31)$$

$$\begin{aligned} \sigma_{\text{non-bs}}(0) &= \frac{e^2}{16\pi^2\hbar} (1+R^2)^2 \\ &\times \int_0^\infty dx \text{Tr} \left[(K_x \Pi K_x^T + K_x^T \Pi K_x) A_x (\mathcal{I} - A_x)^{-1} \right]. \end{aligned} \quad (32)$$

Here the matrices A_x , \tilde{A}_x and K_x are obtained from A_N , \tilde{A}_N and K_N ($N \gg 1$) by substitutions [29]:

$$P_N \rightarrow \frac{1}{\sqrt{x + (1 + \tau/\tau_\phi)^2}}, \quad P_N^{(m)} \rightarrow \frac{(\sqrt{1+x}-1)^m}{x^{m/2}\sqrt{1+x}}. \quad (33)$$

The zero-field conductivity correction is presented in Fig. 2. Figure 2(a) demonstrates that the backscattering and non-backscattering contributions compensate each other to a large extent. The total correction depends, however, on the Fermi level position at $0 < R < 1$. The correction saturates at a certain value after the Fermi level crosses the Dirac point, at $R \geq 1$, Sec. III B.

In the diffusion approximation, for $\ln(\tau_\phi/\tau) \gg 1$, we obtain from Eq. (31) the singular contribution from $x \ll 1$:

$$\sigma_{\text{bs}}^{(\text{diff})}(0) = \frac{e^2}{4\pi^2\hbar} \frac{1+3R^2}{1+R^2} \ln\left(\frac{\tau_\phi}{\tau}\right), \quad (34)$$

and similarly from Eq. (32):

$$\sigma_{\text{non-bs}}^{(\text{diff})}(0) = -\frac{e^2}{2\pi^2\hbar} \frac{R^2}{1+R^2} \ln\left(\frac{\tau_\phi}{\tau}\right). \quad (35)$$

Therefore, the result of the diffusion approximation in zero field is independent of the Fermi level position:

$$\sigma_{\text{total}}^{(\text{diff})}(0) = \frac{e^2}{4\pi^2\hbar} \ln\left(\frac{\tau_\phi}{\tau}\right). \quad (36)$$

The zero-field correction in the diffusion approximation is independent of R as it should be in a system belonging to a symplectic class of symmetry. This is not the case for exact results accounting for ballistic contributions, see Fig. 2. This difference is caused by the interference corrections from ballistic trajectories with a few scatterers (three or more, because we discuss the contribution sensitive to magnetic field). These processes, taken into account in the exact calculation, are regular at low τ/τ_ϕ . Therefore, we have

$$\sigma(0) = \sigma_{\text{total}}^{(\text{diff})}(0) + \sigma_{\text{ball}}(0). \quad (37)$$

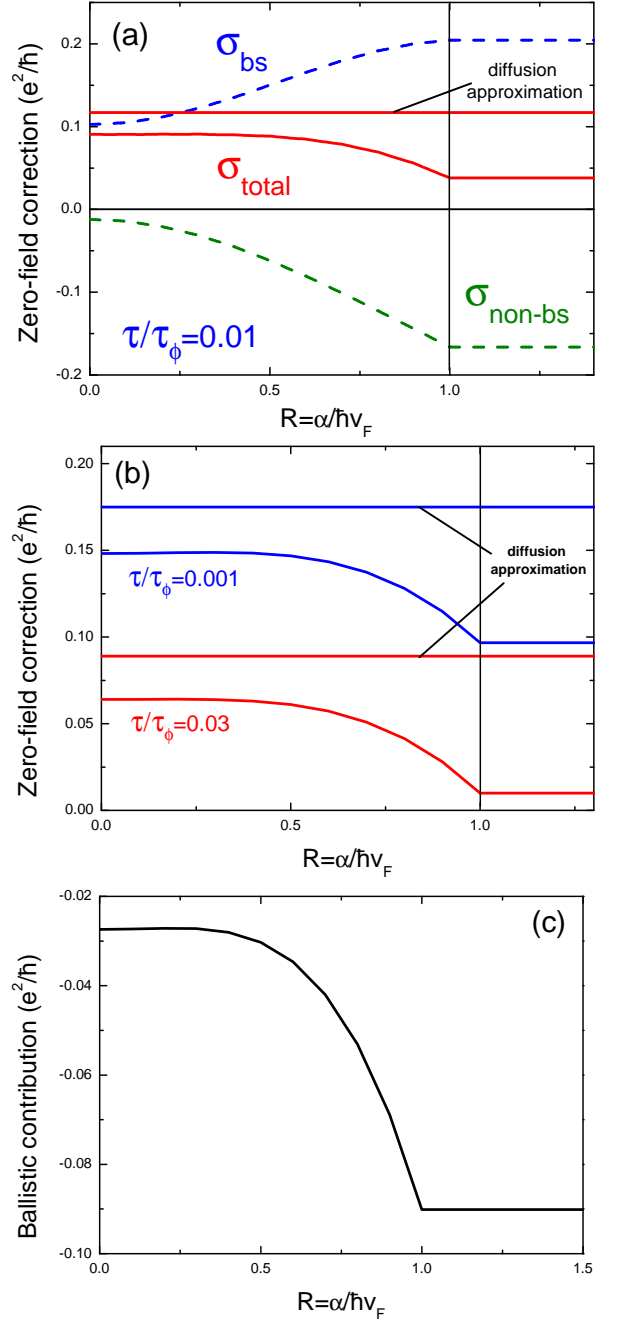


FIG. 2. Zero field conductivity correction as a function of the Rashba splitting parameter $R = \alpha/(\hbar v_F)$. Dashed lines in panel (a) represent the backscattering and the non-backscattering contributions to the total conductivity correction. Panel (c) represents the ballistic contribution $\sigma_{\text{ball}}(0)$ for $\tau/\tau_\phi \ll 1$.

While the first term here is the diffusive contribution (36) independent of R , the second term is a ballistic contribution independent of τ_ϕ . The correction $\sigma_{\text{ball}}(0)$ determines the dependence of the total conductivity correction on the spin-orbit splitting. This function, shown in Fig. 2(c), demonstrates an essential role of ballistic pro-

cesses in weak localization.

The magnetic-field dependence of the conductivity correction is shown in Fig. 3. The magnetic field is given in units of the “transport” field

$$B_{tr} = \frac{\hbar}{2el^2}. \quad (38)$$

The correction monotonously decreases with the magnetic field for all R . The magnetoconductivity varies with the Rashba splitting. The magnetic field dependence is stronger at low R due to higher zero-field values of the correction.

In high magnetic fields $B \gg B_{tr}$ (but still B is classically weak), the conductivity correction decreases according to the following asymptotic law:

$$\sigma_{hf} = \frac{e^2}{\hbar} \lambda \sqrt{\frac{B_{tr}}{B}}. \quad (39)$$

The coefficient λ is a sum of backscattering and non-backscattering contributions, $\lambda = \lambda_{bs} + \lambda_{non-bs}$, where

$$\lambda_{bs} = -\frac{1 + 3R^2}{\sqrt{2}\pi^2} \sum_{N=0}^{\infty} \text{Tr} \left(\Pi \tilde{A}'_N A'_N{}^2 \right), \quad (40)$$

$$\lambda_{non-bs} = \frac{(1 + R^2)^2}{2\sqrt{2}\pi^2} \times \sum_{N=0}^{\infty} \text{Tr} \left(K'_N \Pi K'_N{}^T A'_N + K'_N{}^T \Pi K'_N A'_{N+1} \right). \quad (41)$$

The primed matrices are obtained from A_N , \tilde{A}_N and K_N by the following substitutions [25]: all $P_N^{(m)}$ with odd N should be taken by zeros, and at even $N = 2k$

$$P_{2k} \rightarrow \sqrt{\frac{\pi}{2}} \frac{(2k)!}{2^{2k} (k!)^2}, \quad P_{2k}^{(2)} \rightarrow \sqrt{\frac{\pi}{2}} \frac{\sqrt{(2k)!} (2k+2)!}{2^{2k+1} k! (k+1)!}, \quad (42)$$

$$P_{2k}^{(1)} \rightarrow -\frac{1}{\sqrt{2k+1}}, \quad P_{2k}^{(3)} \rightarrow -\sqrt{\frac{2k+2}{(2k+1)(2k+3)}}.$$

Dependencies of the coefficients λ , λ_{bs} and λ_{non-bs} on R are shown in the inset to Fig. 3. The high-field asymptotes Eq. (39) are presented in Fig. 3 by dashed lines. Comparison with the results of exact calculation shows that the asymptotes describe the conductivity correction in reasonably weak fields for small R only. For $R > 0.3$ the asymptotic dependence (39) is achieved at $B \geq 100B_{tr}$, and only the exact expressions describe the magnetoconductivity in classically weak fields.

The magnetoconductivity in the diffusion approximation is given by the conventional expression for systems with fast spin relaxation:

$$\sigma_{total}^{(diff)}(B) - \sigma_{total}^{(diff)}(0) = -\frac{e^2}{4\pi^2\hbar} f_2 \left(\frac{B}{B_{tr}} \frac{\tau}{\tau_\phi} \right), \quad (43)$$

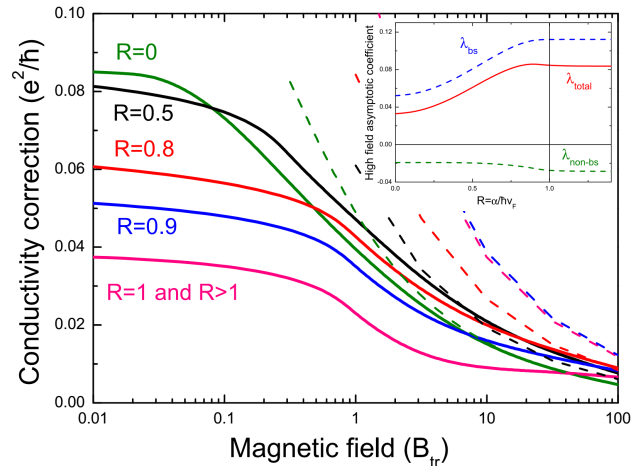


FIG. 3. Magnetoconductivity at different $R = \alpha/(\hbar v_F)$. The dephasing rate $\tau/\tau_\phi = 0.01$. Dashed lines present the high-field asymptotics Eq. (39). Inset: coefficient λ (solid line) and λ_{bs} , λ_{non-bs} (dashed lines).

where $f_2(x) = \psi(1/2 + 1/x) + \ln x$. It is well known that the diffusion approximation does not describe the magnetoconductivity in fields $B \gtrsim B_{tr}$ [11, 28]. Moreover, in the studied system with large spin-orbit splitting, the diffusion approximation for the magnetoconductivity does not capture the dependence of conductivity on R .

While zero-field values of the correction are maximal at $R = 0$, Fig. 2, the inset and asymptotes in Fig. 3 show that at $R = 0$ the correction tends to zero faster than at $R > 0$. Therefore our calculations demonstrate that the total magnetic-field dependent correction is maximal at Fermi level far above the Dirac point.

V. CONCLUSION

In the present work we have developed the theory of weak localization in 2D systems with a strong linear-in- \mathbf{k} spin-orbit splitting of the energy spectrum. The theory describes weak antilocalization in systems with the Rashba or Dresselhaus isotropic spin-orbit splittings. Both ballistic trajectories with few scattering events and long diffusive trajectories are taken into account. It is shown that in the ballistic case the backscattering and the non-backscattering contributions to the conductivity have the same order of magnitude and different signs compensating each other to a large extent. The ballistic contribution to the conductivity correction is found to depend on the spin-orbit coupling in contrast to results of the diffusion approximation. The obtained expressions for the zero-field conductivity correction describe the non-interacting part of its temperature dependence. In this paper, we have considered scattering off the short-range disorder. For smooth scattering potential, the correction depends on the Fermi energy even for the Fermi

level below the Dirac point. In order to derive the magnetoconductivity for this case, one should, however, choose a concrete form of the scattering potential because the Cooperon depends on all Fourier harmonics of the elastic scattering probability.

To conclude, we have derived analytical expression for the conductivity correction that includes both diffusive and ballistic contributions and is valid in a wide interval of the phase breaking rates and magnetic fields. We have also found that the ballistic contribution depends solely on the spectrum characteristics and, therefore, reflects intrinsic properties of the system, which are insensitive

to the details of the scattering and dephasing.

ACKNOWLEDGMENTS

We thank M. O. Nestoklon for helpful discussions. Partial financial support from the Russian Foundation for Basic Research, the EU Network FP7-PEOPLE-2013-IRSES Grant No 612624 “InterNoM”, by Programmes of RAS, and DFG-SPP1666 is gratefully acknowledged.

-
- [1] B. L. Altshuler and A. G. Aronov, in *Electron-Electron Interactions in Disordered Systems*, edited by A. L. Efros and M. Pollak, (Elsevier, Amsterdam, 1985).
 - [2] G. Bergmann, *Phys. Rep.* **107**, 1 (1984).
 - [3] V. F. Gantmakher, *Electrons and Disorder in Solids*, transl. by Lucia I. Man, International Series of Monographs on Physics **130** (Oxford University Press, 2005).
 - [4] S. V. Iordanskii, Yu. B. Lyanda-Geller, and G. E. Pikus, *Pisma Zh. Eksp. Teor. Fiz.* **60**, 199 (1994) [*JETP Lett.* **60**, 206 (1994)].
 - [5] W. Knap, C. Skierbiszewski, A. Zduniak, E. Litwin-Staszewska, D. Bertho, F. Kobbi, J. L. Robert, G. E. Pikus, F. G. Pikus, S. V. Iordanskii, V. Mosser, K. Zekentes, and Yu. B. Lyanda-Geller *Phys. Rev. B* **53**, 3912 (1996).
 - [6] G. M. Minkov, A. V. Germanenko, O. E. Rut, A.A. Sherstobitov, L. E. Golub, B. N. Zvonkov and M. Willander, *Phys. Rev. B* **70**, 155323 (2004).
 - [7] V. M. Gasparyan and A. Yu. Zyuzin, *Fiz. Tverd. Tela (Leningrad)* **27**, 1662 (1985) [*Sov. Phys. Solid State* **27**, 999 (1985)].
 - [8] M. I. Dyakonov, *Solid State Commun.* **92**, 711 (1994).
 - [9] A. P. Dmitriev, V. Yu. Kachorovskii, and I. V. Gornyi, *Phys. Rev. B* **56**, 9910 (1997).
 - [10] S. McPhail, C. E. Yasin, A. R. Hamilton, M. Y. Simmons, E. H. Linfield, M. Pepper, and D. A. Ritchie *Phys. Rev. B* **70**, 245311 (2004).
 - [11] L. E. Golub, *Phys. Rev. B* **71**, 235310 (2005).
 - [12] M.M. Glazov and L.E. Golub, *Semicond. Sci. Technol.* **24**, 064007 (2009).
 - [13] D. Spirito, L. Di Gaspere, F. Evangelisti, A. Di Gaspere, E. Giovine, and A. Notargiacomo, *Phys. Rev. B* **85**, 235314 (2012).
 - [14] I. S. Lyubinskiy and V. Yu. Kachorovskii *Phys. Rev. B* **70**, 205335 (2004); *Phys. Rev. Lett.* **94**, 076406 (2005).
 - [15] S. D. Ganichev and L. E. Golub, *Phys. Status Solidi B* **251**, 1801 (2014).
 - [16] M. Sakano, M. S. Bahramy, A. Katayama, T. Shimojima, H. Murakawa, Y. Kaneko, W. Malaeb, S. Shin, K. Ono, H. Kumigashira, R. Arita, N. Nagaosa, H. Y. Hwang, Y. Tokura, and K. Ishizaka, *Phys. Rev. Lett.* **110**, 107204 (2013).
 - [17] H. Liang, L. Cheng, L. Wei, Z. Luo, G. Yu, C. Zeng, and Z. Zhang, *Phys. Rev. B* **92**, 075309 (2015).
 - [18] G. M. Minkov, A. V. Germanenko, O. E. Rut, A. A. Sherstobitov, S. A. Dvoretzki, and N. N. Mikhailov, *Phys. Rev. B* **89**, 165311 (2014).
 - [19] V. Brosco, L. Benfatto, E. Cappelluti, and C. Grimaldi, arXiv:1506.01944 (2015).
 - [20] I. V. Gornyi, A. P. Dmitriev, and V. Yu. Kachorovskii, *JETP Lett.* **68**, 338 (1998).
 - [21] M. A. Skvortsov, *JETP Lett.* **67**, 133 (1998); arXiv:cond-mat/9712135v2.
 - [22] G. Tkachov and E. M. Hankiewicz, *Phys. Rev. B* **84**, 035444 (2011).
 - [23] V. Krueckl and K. Richter, *Semicond. Sci. Technol.* **27**, 124006 (2012).
 - [24] P. M. Ostrovsky, I. V. Gornyi, and A. D. Mirlin, *Phys. Rev. B* **86**, 125323 (2012).
 - [25] I. V. Gornyi, V. Yu. Kachorovskii, and P. M. Ostrovsky, *Phys. Rev. B* **90**, 085401 (2014).
 - [26] I. V. Gornyi, V. Yu. Kachorovskii, A. D. Mirlin, and P. M. Ostrovsky, *Phys. Status Solidi B*, **251**, 1786 (2014).
 - [27] M. I. Dyakonov and V. Yu. Kachorovskii, *Fiz. Tekh. Poluprovodn.* **20**, 178 (1986) [*Sov. Phys. Semicond.* **20**, 110 (1986)].
 - [28] M. O. Nestoklon, N. S. Averkiev, S. A. Tarasenko, *Solid State Commun.* **151**, 1550 (2011).
 - [29] M. O. Nestoklon and N. S. Averkiev, *Phys. Rev. B* **90**, 155412 (2014).